ARTICLE

OBC
www.rsc.org/obc

Synthesis and spectroscopy of an oligophenyl based cruciform with remarkable π–π assisted folding†

Benjamin S. Nehls,[a] Frank Galbrecht,[a] Askin Bilge,[a] David J. Brauer,[b] Christian W. Lehmann,[c] Ullrich Scherf*[a] and Tony Farrell*[a]

[a] *Bergische Universität Wuppertal, Institut für Polymertechnologie, Makromolekulare Chemie, Gauss-Str. 20, D-42097 Wuppertal, Germany*
E-mail: scherf@uni-wuppertal.de, farrell@uni-wuppertal.de; Fax: 49 202 439 3880; Tel: 49 202 439 2493

[b] *Bergische Universität Wuppertal, Anorganische Chemie, Gauss-Str. 20, D-42097 Wuppertal, Germany*

[c] *Max-Planck-Institut für Kohlenforschung, Kaiser-Wilhelm-Platz 1, D-45470 Mühlheim an der Ruhr, Germany*

Received 8th June 2005, Accepted 19th July 2005
First published as an Advance Article on the web 2nd August 2005

A facile route has been developed for the preparation of a new family of oligophenyls based on a 2,5,2′,5′-tetra-aryl substituted biphenyl structural motif. The cruciform terphenyl dimer 2,5,2′,5′-tetra(4-*tert*-butylphenyl)-1,1′-biphenyl (**2**) has been prepared in a two step protocol as a representative of this interesting class of materials. The thermal behaviour of the cruciform was analysed by DSC and shows that **2** forms an amorphous glass when cooled from the isotropic melt. Subsequent heating reveals a glass transition temperature at 130 °C. X-Ray single crystal structure analysis of 2,2′-bis(4-*tert*-butylphenyl)-1,1′-biphenyl (**4**) and **2** shows that both these molecules with a quater-phenyl substructure adopt a folded solid-state structure. Examining the ^{1}H NMR spectra of **2** and **4** reveals that the interactions that induce this folding in the solid-state are sufficiently strong to bias foldamer formation also in solution. Consequently, it is reasonable to assume that the folded conformation within the lattice is due to intramolecular π–π interaction rather than being imposed by crystal packing. The optical properties of the cruciform terphenyl dimer **2** are discussed relative to the linear analogue 1,4-bis(4-*tert*-butylterphenyl)benzene (**3**).

Introduction

Organic based π-conjugated materials are expected to be viable components in a diverse range of optoelectronic devices including organic field-effect transistors (OFETs),[1] electroluminescent diodes (OLEDs),[2] lasers[3] and photovoltaic cells.[4] Phenylene based polymers and oligomers are an intensively studied class of conjugated materials due to their excellent thermal and chemical stability.[5] Furthermore, their optical properties make them especially promising candidates as efficient blue emitters in electroluminescent devices and organic solid-state lasers.[6] Although initial investigations concentrated on the design of soluble polymeric materials, lately research has intensified in the oligomer approach.[7] Unfortunately, with increasing chain length oligophenyls exhibit extremely low solubility. On the other hand, an advantage of the small molecule approach is that standard purification techniques result in facile removal of impurities and ill-defined end groups. Moreover, knowledge of the exact constitution and conformation of oligomers allows precise structure–property correlations to be deduced.

It has recently become clear that the subject of nanoscopic and macroscopic order in π-conjugated systems is extremely important, as it is the solid-state morphology that determines the efficiency of electronic or optoelectronic devices. Recent findings have shown that it is often advantageous to apply amorphous materials *e.g.* for OLED applications, as aggregates tend to promote non-radiative recombination processes.[8] Such processes represent a serious drawback in organic based light emitting diodes and solid-state laser applications. Conversely, efficient intermolecular interaction can greatly enhance the charge carrier mobility. Accordingly, polymers and oligomers that encourage substantial intermolecular π–π overlap are often excellent charge transporting components for OFETs. Therefore, to be able to control the spatial orientation and packing of both oligomers and polymers when they assemble in the solid state is a worthwhile, although non-trivial endeavour. This in turn is dependent on the proficiency of the chemist to design and prepare structurally defined π-architectures and correlate the solid-state morphology to the chemical structure.

According to Shirota, disrupting the capacity of a material to planarize enhances the likelihood of glass formation.[8] Moreover, a shape that discourages crystallisation or prevents strong intermolecular packing should in general enhance the solubility. Representative topologies of such molecular glasses include starburst structures,[9,10] spiro-type[11] and tetra-phenylmethane based oligomers.[12] In this contribution we describe a new and efficient synthetic strategy for the construction of cruciform π-conjugated oligomers based on the 2,5,2′,5′-tetra-aryl substituted-1,1′-biphenyl core.

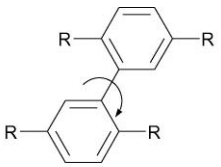

2,5,2',5'-tetra-arylsubstituted-1,1'-biphenyl core

To date the number of publications, which include crystallographic data of related *ortho*-oligoaryls that adopt helical or folded pattern solid-state patterns are still relatively meagre.[13] Significantly though, the question as to whether intramolecular π–π stacking rather than crystal packing biases some of these *ortho*-quateraryls towards foldamer formation has not been unequivocally communicated. To our knowledge, no previous study has probed the solution conformation of

† Electronic supplementary information (ESI) available: full analytical details (Figs. S1–S9). See http://dx.doi.org/10.1039/b508125d

DOI: 10.1039/b508125d

ortho-quateraryls. Such solution data would be very useful to identify the driving forces, which induce torsionally flexible molecules to adopt a folded structure. However, in the case where signal assignment is possible, a ^{1}H NMR study is ideal for a reliable elucidation of the structure in solution. Herein, we show that our cruciform dimers exhibit a coiled conformation both in the solid-state and in solution and that the driving forces for foldamer formation are in fact π-related.

Results and discussion

Synthesis

The key step in the synthesis of the cruciform structure utilizes the different reactivity of bromo and chloro groups in a Suzuki-type aryl–aryl coupling reaction. Thus the reaction of 2.4 equivalents of 4-*tert*-butylbenzene boronic acid with 1,4-dibromo-2-chlorobenzene allows a selective coupling between the two bromo groups and the boronic acid moiety leaving the chloro group in place for further reactions (Fig. 1). The reaction was carried out using a microwave assisted protocol utilizing $Pd(Ph_3)_2Cl_2$ as the catalyst and powdered KOH as the base.[14] The solid material was weighed into a 10 mL vial and then sealed under argon with an aluminium cap containing a septum. THF was then added and the reaction mixture was heated for 10 minutes using microwaves (300 W). A maximum temperature setting of 110 °C was employed and maintained automatically by the microwave set-up.[15] Purification of the chloro-substituted cruciform precursor 1-chloro-2,5-bis(4-*tert*-butylphenyl)benzene (**1**) was accomplished by column chromatography to give **1** in 95% yield.

The cruciform terphenyl dimer 2,5,2′,5′-tetra(4-*tert*-butylphenyl)-1,1′-biphenyl (**2**)[16] was readily available *via* a Nickel-mediated Yamamoto type coupling of **1**.[17] Again the reaction was expedited using microwave heating (300 W) for 12 minutes.[18] Maximum power was applied for the full duration of the reaction and the temperature increased to *ca.* 220 °C. The pure cruciform **2** was realised in 82% yield after column chromatography. Two model compounds were synthesised in order to assist with the structural and optical characterisations of the cruciform molecule. Hence using a microwave-assisted Suzuki coupling the linear oligophenylene 1,4-bis(4-*tert*-butylphenyl)benzene (**3**) and the *ortho*-quaterphenyl compound 2,2′-bis(4-*tert*-butylphenyl)-1,1′-biphenyl (**4**) were prepared from the reaction of 4-*tert*-butylbenzene boronic acid with 1,4-dibromo-benzene and 2,2′-dibromo-1,1′-biphenyl respectively.

X-Ray crystallography

The crystal structures of **2** and **4** have been elucidated from single crystals obtained from solutions of dichloromethane and THF respectively, and the crystallographic details are given in the experimental section. Analysis of the molecular structures of **2** and **4** reveals that both adopt a folded helical conformation, which is characterised by an almost parallel orientation of the terminal phenyl rings combined with a partial overlap. The helical conformation of **2** and **4** is not continued within the crystal packing of the molecules and no noteworthy intermolecular contacts are found. The molecular coordination number[18] is ten for the molecules of **2**, which are situated on a two-fold crystallographic symmetry axis while each

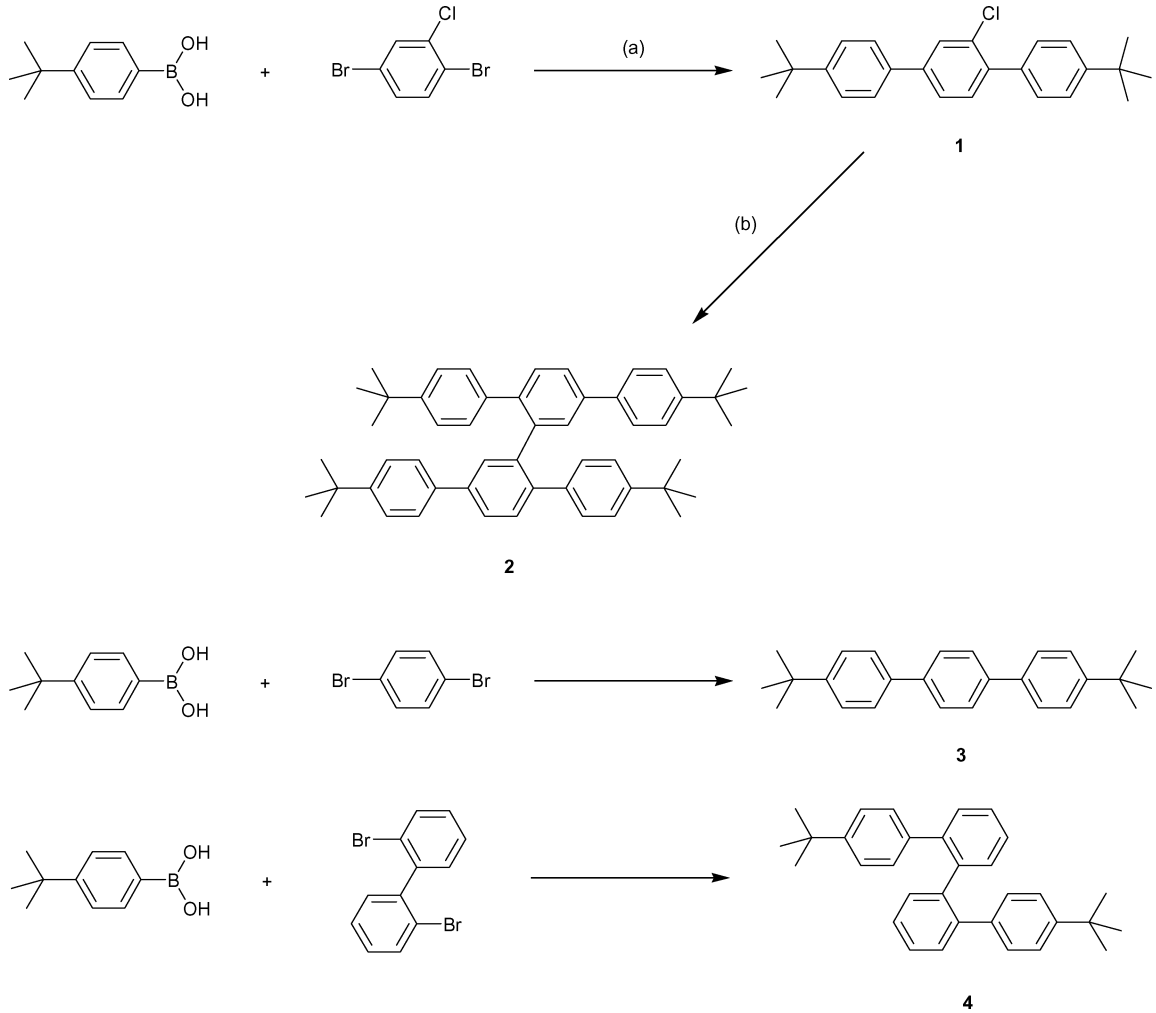

Fig. 1 Reagents and synthetic conditions: (a) $Pd(PPh_3)_2Cl_2$, solid KOH in THF, μW (300 W), 10 min, (temp. ~120 °C); (b) $Ni(COD)_2$ in toluene/DMF, μW (300 W), 10 min, (temp. ~220 °C).

molecule of **4** lies within contact range of twelve neighbouring molecules. The *ortho*-quaterphenyl **4** is a substructure of the cruciform **2** and consequently it is of interest to see how the conformational features of these substructures vary in different packing environments.

Of particular interest are the inter-ring distances between the offset phenyl rings of the C11 and C11′ atoms in **2** and of the C11 and C41 atoms in **4**. Offset parallel geometries are believed to be favourable for π–π interactions.[19] From among the various geometric descriptors for π–π interactions the present work utilises atom–atom contacts and centroid–mean plane distances, rather than ring–centroid to ring–centroid distances. In terms of the cut-off criterion for π-stacking, atom–atom distances <3.6 Å are considered as relatively strong π–π interactions.[20] However, it should be noted that a purely geometrical analysis of intermolecular distances is only an indirect measure of electronic interactions.[19–21]

The two perspectives of **2** illustrated in Fig. 2 show that its above-mentioned phenyl rings are more or less parallel with a dihedral angle of 6.5° formed by their planes. The closest approach between these rings is C11–C11′ [3.1646(17) Å] with an additional six separations in the range 3.4–3.6 Å (3.4 Å being the van der Waals diameter of a carbon atom). There is substantial overlap between the two *tert*-butyl substituted phenyl rings [(C11–C16) and (C11′–C16′)] in **2** with the interplanar distance between them being 3.34 Å. This is defined as the shortest distance between the ring centroid of one ring and the least squares plane of the other ring.

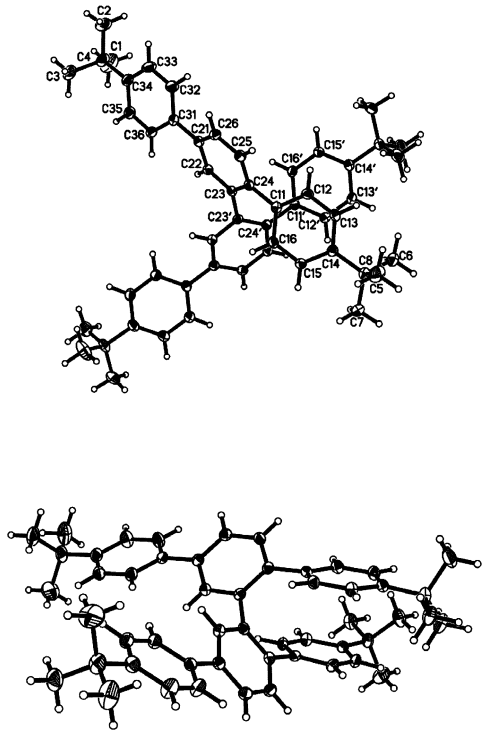

Fig. 2 Two perspective views of the molecular structure of compound **2**. In addition to the values given in the text, the dihedral angle between the ring planes formed by C11 to C16 and C21 to C26 is 44.8°, and between the planes formed by C21 to C26 and C21′ to C26′ is 62°.

In the crystal structure of **4** there is again considerable overlap between the homologous 4-*tert*-butylphenyl units (C11–C16) and (C41–C46) and the interplanar distances between the respective π-systems are 3.30 and 3.46 Å (Fig. 3). The planes of these phenyl rings of **4** are distinctly less parallel (dihedral angle 16.1°), but the shortest contact between them [C11–C41, 3.1379(14) Å] compares well with that of **2**. In accord with the ring planes in **4** being more splayed than those of **2**, the number of additional inter-ring C–C distances less than 3.6 Å is reduced to four as compared to six in **2**. The reduced ring slippage and

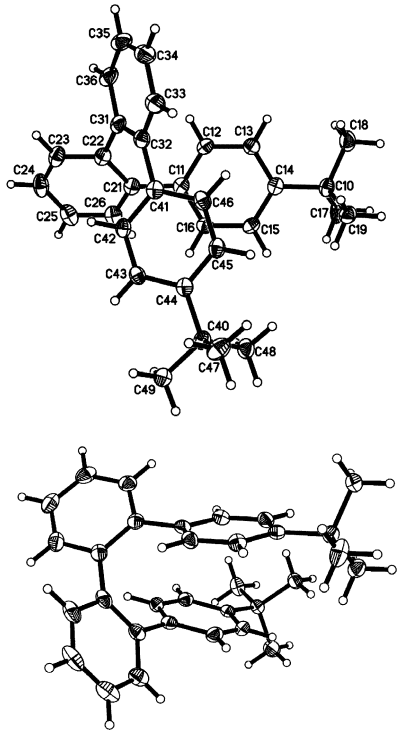

Fig. 3 Two perspective views of the molecular structure of compound **4**. The planes formed by C11 to C16 and C21 to C26 intersect at 44.1°. The dihedral between C21 to C26 and C31 to C36 is 56.4° and the dihedral angle between C31 to C36 and C41 to C46 is 47.2°.

tilt in **2** is accompanied by increased twisting in the central biphenyl moiety. Thus, the C21–C22–C31–C32 torsion angle in **4** is 6.6(3)° smaller than the corresponding torsion angle value of **2** [C24–C23–C23′–C24′, 63.0(2)°].

NMR spectroscopy

The compounds **2–4** display good solubility in common organic solvents, which allowed a detailed characterisation of the materials by NMR spectroscopy. Fig. 4 shows the aromatic region of the proton NMR spectrum of the terphenyl dimer **2** and the model *ortho*-quaterphenyl compound **4**. The most notable feature in both spectra is the high-field position of two directly coupled doublets. For **4** they are found at δ = 6.34 and 6.87 ppm with a coupling constant of 8.2 Hz and represent the four protons of the 4-*tert*-butylphenyl units. This kind of shielding effect has been observed in conformationally rigid carbohelicenes and is due to the increased overlap of the aromatic rings.[22] A similar upfield shift of the aromatic protons has been reported in fluorenyl substituted flexible polyolefins in which the fluorene side-chain units adopt a cofacial arrangement and is supported with X-ray crystallographic data.[23] Well-defined conformations have also been achieved using a variety of flexible oligomers by means of solvophobic, electrostatic, hydrogen bonding and metal–ligand interactions.[24] In view of

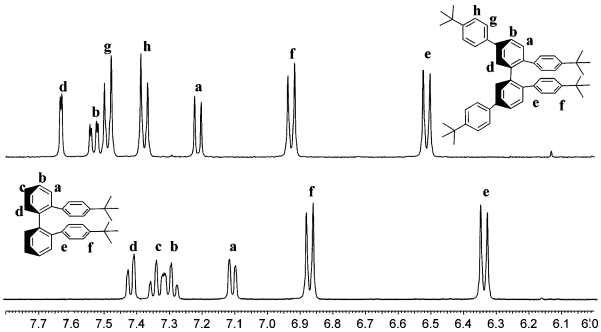

Fig. 4 ^{1}H NMR spectra of **2** and **4** in $C_2D_2Cl_4$.

this we propose that the *ortho*-quaterphenyl **4** also forms a folded conformation in solution, wherein the outer *tert*-butylphenyls adopt an offset π-stacked arrangement (see inset Fig. 4). This intrinsic tilted-displaced pattern most probably originates from the strong σ–π attraction between the protons of one *tert*-butylphenyl unit and its homologous neighbour. A slight tilt between the corresponding *tert*-butylphenyl rings results in a larger upfield shift of the two protons (labelled "e" in Fig. 4) closest to the central biphenyl unit. A 2D ROESY spectrum illustrates the through space connectivity between the upfield doublet at $\delta = 6.34$ ppm and the peak at $\delta = 6.87$ ppm and validates the proposed π-stacked conformation.† Analysis of the ^{1}H NMR and correlated NMR spectra† allows a full assignment of the structure based on the proposed coiled conformation and is presented in Fig. 4. This implies that the internal driving forces that predispose the conformational dynamics of the molecule to favour a folded helical type conformation in the solid-state result from π-related intramolecular interactions.

The similarities between the ^{1}H NMR spectra of **4** and **2** suggest that the cruciform molecule **2** likewise adopts a folded conformation in solution. For example, the ^{1}H NMR spectrum of **2** again shows a pair of coupled high field doublets at $\delta = 6.51$ and 6.93 ppm due to the increased overlap of the two *tert*-butylphenyl rings. The spatial proximity between the upfield doublet at $\delta = 6.51$ ppm and the proton signal H_a at $\delta = 7.21$ ppm from the central tetra-substituted biphenyl unit is manifested by the strong coupling between the signals in the 2D ROESY spectrum of **2** (Fig. 5). Analysis of the ^{1}H–^{1}H COSY, ^{1}H–^{1}H COSYLR and the ROESY spectra of **2** allows an unambiguous assignment of all the protons in the molecule (see inset Fig. 4).† Additionally, a study of the effect of temperature on the solution conformation was conducted by variable temperature (VT) ^{1}H NMR.† Up to 70 °C the pattern remained symmetrical and relatively unchanged demonstrating the robustness of the interaction. As expected, upon cooling to a temperature of −50 °C the highfield doublets become broader and are shifted even further upfield by ~0.2 ppm due to a slowing of the molecular dynamics.

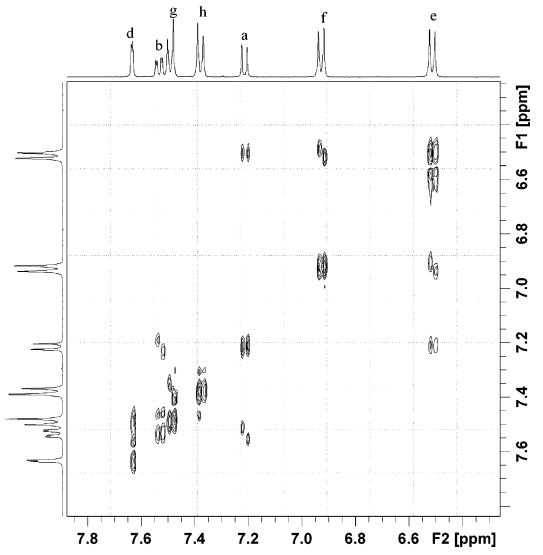

Fig. 5 ^{1}H–^{1}H ROESY NMR spectrum of **2** in $C_2D_2Cl_4$.

Thermal properties

Thermal stability and high glass transition temperatures (T_g) are prerequisites when considering amorphous materials as components for electronic and optoelectronic devices as OLED degradation is often linked with morphological changes within the active organic material. The thermal behaviour of the oligomers **2** and **4** was analysed by differential scanning calorimetry (DSC) in the temperature range from −20 °C to 300 °C with heating and cooling rates of 10 °C min^{-1}. The DSC curves for a recrystallised sample of **4** are presented in Fig. 6. During the first cycle an endothermic peak due to melting was observed at 97 °C. When the isotropic liquid was subsequently cooled a glass was spontaneously formed with a T_g at 25 °C. The resulting glass sample is morphologically stable and in the successive heating cycles no recrystallisation occurred upon heating well above the melting point. In the heating cycles a constant T_g at 28 °C is observed.

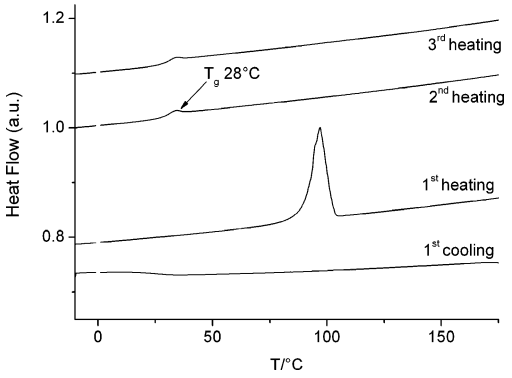

Fig. 6 DSC traces for **4**.

The DSC traces for a recrystallised sample of the cruciform terphenyl dimer **2** are shown in Fig. 7. The first heating curve displays only one endothermic peak at 275 °C which is assigned to the transition into the isotropic melt. Analogous to the *ortho*-quaterphenyl compound **4** only a T_g at 128 °C is observed in the following cooling cycle. The subsequent heating cycles of the cruciform structure **2** display quite marked differences to the quaterphenyl derivative compound **4**. First, the T_g of **2** is over one hundred degrees higher than that of **4** but the larger molecule displays a greater tendency to recrystallise. The second heating curve not only shows a T_g at 135 °C but also an endothermic recrystallisation peak at ~248 °C followed by the melting transition at 276 °C. This thermal behavior is reproducible even after several repeated cycles. Although the glassy state formed from the isotropic melt is not stable at temperatures above 200 °C the T_g is already quite high. We expect that further modifications to the oligophenyl will result in a higher T_g and suppress recrystallisation. Variations already in progress include: extending the length of the arms, introducing substituents which induce intermolecular interactions such as hydrogen bonding or dipolar interactions and the incorporation of the structurally more rigid 9,9′-dialkylfluorene unit.

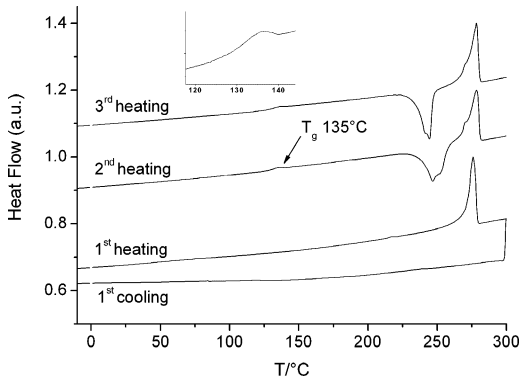

Fig. 7 DSC traces for **2**. The inset shows the T_g area.

Optical spectroscopy

While the crystallographic data reflect the solid-state structure of the material, the optical properties mirror the interplay between the molecular structure and the electronic properties.

Table 1 Photophysical data for the cruciform **2** and the linear terphenyl **3**

	Absorption/nm			PL/nm[b]		Stokes shift[c]
Entry	$CHCl_3$[a]		Film	$CHCl_3$	Film	$1/\lambda_{max} - 1/\lambda_{em}$
2	281	(53 800)	277	394	406	10 200
3	287	(33 800)	280	336	356	5 100

[a] Extinction coefficient in brackets (M^{-1} cm^{-1}). [b] Film excited at absorption λ_{max}. [c] Calculated from the solution values.

The optical spectra of the cruciform terphenyl dimer **2** and the linear terphenyl analogue **3** were examined both in dilute solution and as spin cast film and the data are presented in Table 1. The optical properties of the chromophore **3** are typical of *para*-oligophenylenes in general.[25]

The absorption spectrum is broad and featureless with a maximum (λ_{max}) at 287 nm (Fig. 8). This may indicate that the chromphore adopts an essentially non-planar ground state configuration due to the strong steric hindrance between the phenyl rings. The solution PL spectrum on the other hand (Fig. 8) is more resolved and displays the 0–0 emission maximum (λ_{em}) at 336 nm accompanied by vibronic side bands at 352 and 368 (sh) nm. These optical band features are characteristic of chromophores that adopt a more planar arrangement upon photexcitation due to an increased bond order of the exocyclic phenyl–phenyl bonds. In agreement with a large topology change between the ground and excited states, compound **3** exhibits a relatively large Stokes shift of 5 100 cm^{-1} (calculated from $1/\lambda_{max} - 1/\lambda_{em}$). The solid-state optical features of **3** are similar to those in solution. The absorption band shape remains featureless and the λ_{em} is red-shifted by only 20 nm. Such minor differences in the optical properties are commonly associated with a change in the environment on going from solution to the film.

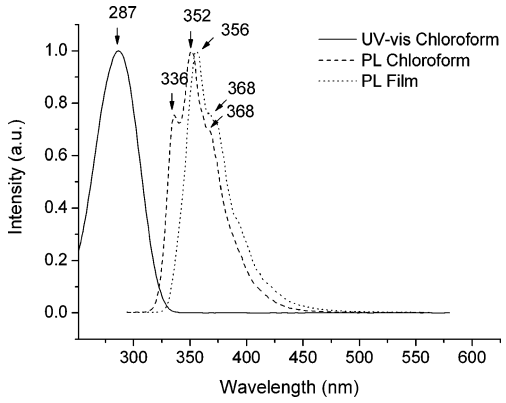

Fig. 8 Absorption and PL spectra of **3**.

A comprehensive study by Berlman *et al.* on the electronic spectra of oligophenyls illustrated that subtle changes in the substitution patterns of alkyls along the chromophore backbone can have dramatic effects on the spectroscopic properties.[25] Her results indicated that alkyl substitution on the central phenyl ring of *para*-terphenyls results in substantial disturbance to the planarity of the chromophore. The signatures of these steric effects include: (i) a blue-shift of the λ_{max}, (ii) a reduction in the extinction coefficient, (iii) a broader and less structured fluorescence spectrum and (iv) an increased Stokes shift. The optical spectra of the cruciform chromophore **2** are presented in Fig. 9. The absorption spectrum of **2** is broad and structureless and is more or less similar to the linear analogue **3**. The long wavelength absorption maximum is slightly blue-shifted (6 nm) which is consistent with an increase in the distortion within the terphenyl arms in the ground state. On the other hand, there is quite a significant difference between the PL spectra

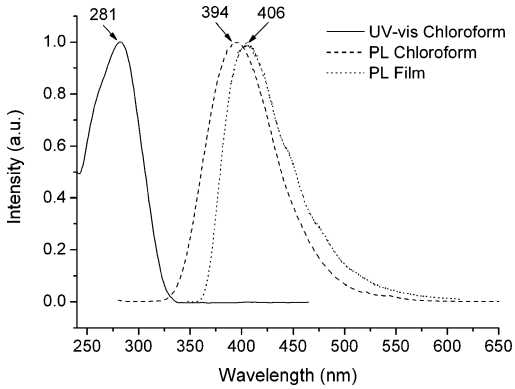

Fig. 9 Absorption and PL spectra of **2**.

of **2** and **3**. The emission maximum of **2** is much broader and bathochromically shifted by *ca.* 60 nm relative to the emission maximum of **3**.

In a first view, the features of the optical spectra of **2** are in agreement with a highly distorted ground-state conformation with a large change in topology upon photoexcitation. However, the NMR data unambiguously illustrate that folding due to the strong intramolecular π–π interaction is not restricted to the solid state of **2**. Regarding this, the larger bathochromic shift of the PL band for the cruciform dimer **2** compared to that of the linear analogue **3** has to be related to these intramolecular π-interactions. As the cruciform **2** clearly has a stacked ground state configuration prior to photoexcitation it is feasible to contend that the λ_{em} band at 394 nm arises from the presence of an intramolecular excited state dimer. The characteristic signature for the formation of excimers is a weak, broad and red-shifted emission. The quantum yield of **2** was obtained in solution and in thin film *versus* anthracene as the standard and gave yields of Φ of 0.13 and 0.06 respectively. This fluorescence intensity is already quite low in solution which lends credence to the formation of excimers due to an interaction between the arms. Curiously however, the cruciform terphenyl dimer **2** exhibits a substantial hyperchromicity of the λ_{max} relative to the *para*-terphenyl **3**. Conversely, hypochromic effects have been reported for π-stacked base pairs in a double helical strand in DNA and additionally for π-stacked polymers.[23a,26] However, the two terphenyl chromophores that form the cruciform **2** are covalently linked, and thus are able to interact electronically, which may explain the observed hyperchromicity. A more in-depth study including time-resolved fluorescence experiments is required to fully elucidate these effects.

Nonetheless, the optical properties of the cruciform terphenyl dimer **2** as a representative of this new family of cruciform oligophenyls make them promising candidates for stimulated emission and lasing experiments due to their large Stokes shift, which eliminates reabsorption effects. At the same time, the fact that **2** already displays a relatively large T_g bodes well for the use of such oligomers as active components for blue-emitting OLEDs. However, it remains to be seen what effect the presence of the stacked ground-state conformation has on the electronic properties.

Conclusion

We have presented an efficient method for the synthesis of 2,5,2′,5′-tetra(4-*tert*-butylphenyl)-1,1′-biphenyl (**2**) as a prototype of a new family of cruciform-type π-systems based on the 2,5,2′,5′-tetra-aryl substituted-1,1′-biphenyl structural motif. Examination of the X-ray structure and ^{1}H NMR data of **2** and the *ortho*-quaterphenyl model compound 2,2′-bis(4-*tert*-butylphenyl)-1,1′-biphenyl (**4**) reveals the presence of strong π-related interactions within these molecules both in solution and in the solid-state. Both **2** and **4** form glassy materials upon cooling the samples from the isotropic melt. For the cruciform *para*-terphenyl dimer **2** the glass transition temperature at *ca.* 130 °C is more than 100 degrees higher than that of the model compound **4**. In solution the oligophenyl **2** absorbs in the ultraviolet region (λ_{max} = 281 nm) while the emission is blue in colour (λ_{em} = 394 nm). The large Stokes is very probably related to the formation of intramolecular excimers as a result of the strong π–π interaction. Ongoing synthetic work involves the synthesis and characterisation of related cruciform oligoaryls with extended arms including 9,9′-dialkylfluorenyl, perfluoroalkylphenyl, 4,4′-dialkyltriphenylamine and 2,5-thienyl units as well as the incorporation of such cruciform oligoaryl building blocks into polymers. Furthermore, theoretical studies are also underway in order to correlate the structure and the optical properties.

Experimental

All reactions were carried out under an argon atmosphere. The solvents were used as commercial p.a. quality. ^{1}H- and ^{13}C-NMR data were obtained on a Bruker ARX 400 spectrometer. Phase transitions were studied by differential scanning calorimetry (DSC) with a Bruker Reflex II thermosystem at a scanning rate of 10 °C min^{-1} for both heating and cooling cycles. The UV–Vis and fluorescence spectra were recorded on a Jasco V-550 spectrophotometer and a Varian-Cary Eclipse spectrometer respectively. Low-resolution mass spectrometry was obtained on a Varian MAT 311A operating at 70 eV (Electron Impact, EI) and reported as *m*/*z* and percentage relative intensity. FD mass measurements were carried out on a ZAB 2-SE-FDP. Microwave assisted synthesis was performed using a CEM-Discovery monomode microwave utilizing an IR-temperature sensor, magnetic stirrer and sealed in 10 mL glass vials with aluminium caps with a septum. All reactions were monitored and controlled using a personal computer.

Synthesis of 1-chloro-2,5-bis(4-*tert*-butylphenyl)benzene (1) *via* a non-aqueous microwave procedure

A dried 10 mL microwave tube was charged with 1-chloro-2,5-dibromobenzene (0.1 g, 0.37 mmol), 4-*tert*-butyl-phenylboronic acid (0.14 g, 0.79 mmol), KOH (0.12 g, 2.14 mmol), $Pd(PPh_3)_2Cl_2$ (0.013 g, 0.02 mmol) and sealed under argon with an aluminium cap with a septum. Dry THF (4 mL) was added *via* a syringe and the reaction was irradiated with microwaves (300 W) for 10 min with air-cooling to keep the temperature between 110 and 115 °C. The mixture was poured into water and then extracted with dichloromethane, which was subsequently washed with water and brine, dried over $MgSO_4$ and the solvent was removed by rotary evaporation. The residue was purified by column chromatography on silica gel with hexanes–ethyl acetate (99 : 1) as eluent to give **1** in 95% yield. ^{1}H NMR (400 MHz, $C_2D_2Cl_4$, 80 °C): δ 7.64 (d, 1H, J = 1.9 Hz), 7.52 (m, 3H), 7.43 (m, 6H), 7.37 (d, 1H, J = 8.0 Hz), 1.34 (s, 9H), 1.33 (s, 9H) ppm. ^{13}C NMR (100 MHz, CD_2Cl_4, 80 °C): δ = 151.3, 150.7, 141.3, 138.9, 136.3, 136.0, 132.9, 132.1, 129.4, 128.4, 126.8, 126.2, 125.5, 125.3, 34.8, 34.8, 31.7, 31.6 ppm. FD-MS: 377.0 (100.0). Elemental analysis calculated for $C_{26}H_{29}Cl$: C, 82.84; H, 7.75. Found: C, 82.81; H, 7.46%.

Synthesis of 2,5,2′,5′-tetra(4-*tert*-butylphenyl)-1,1′-biphenyl (2) *via* a Yamamoto coupling

A dried 10 mL microwave tube was charged with **1** (0.10 g, 0.27 mmol), $Ni(COD)_2$ (109 mg, 0.40 mmol), 2,2′-bipyridyl (62 mg, 0.40 mmol), COD (43 mg, 0.40 mmol) and sealed under argon with an aluminium cap with a septum. Dry DMF (1 mL) and toluene (3 mL) were added *via* a syringe and the reaction was irradiated with microwaves (300 W) for 12 min at a temperature of ~220 °C. The mixture was poured into water and then extracted with dichloromethane. The organic phase was subsequently washed with 2N HCl, water, brine and dried over Na_2SO_4. After the solvent was removed by rotary evaporation the residue was purified by column chromatography on silica gel with hexanes–toluene (95 : 5) as eluent to give **2** in 82% yield. ^{1}H NMR (400 MHz, $C_2D_2Cl_4$, 80 °C): δ 7.63 (d, 2H, J = 1.7 Hz), 7.53 (dd, 2H, J = 8.2, J = 1.8 Hz), 7.49 (d, 4H, J = 8.4 Hz), 7.38 (d, 4H, J = 8.4 Hz), 7.21 (d, 2H, J = 8.1), 6.93 (d, 4H, J = 8.3 Hz), 6.51 (d, 4H, J = 8.5 Hz), 1.29 (s, 18H), 1.23 (s, 18H) ppm. ^{13}C NMR (100 MHz, $C_2D_2Cl_4$, 80 °C): δ 150.7, 148.9, 140.5, 139.8, 139.3, 137.8, 137.5, 130.6, 130.5, 128.9, 126.8, 126.1, 126.0, 124.8, 34.7, 34.5, 31.6 ppm. FD-MS: 682.4 (100.0). Elemental analysis calculated for $C_{52}H_{58}$: C, 91.44; H, 8.56. Found: C, 90.75; H, 8.12%.

Synthesis of 1,4-bis(4-*tert*-butylterphenyl)benzene (3) *via* a non-aqueous microwave procedure

A dried 10 mL microwave tube was charged with 1,4-dibromobenzene (0.06 g, 0.25 mmol), 4-*tert*-butyl-phenylboronic acid (0.105 g, 0.59 mmol), KOH (0.16 g, 2.86 mmol), $Pd(PPh_3)_2Cl_2$ (0.013 g, 0.02 mmol) and sealed under argon with an aluminium cap with a septum. Dry THF (4 mL) was added *via* a syringe and the reaction was irradiated with microwaves (300 W) for 10 min with air-cooling to keep the temperature between 110 and 115 °C. The mixture was poured into water and then extracted with dichloromethane, which was subsequently washed with water and brine, dried over $MgSO_4$ and the solvent was removed by rotary evaporation. The residue was purified by column chromatography on silica gel with hexanes–toluene (97 : 3) as eluent to give **3** in 90% yield. ^{1}H NMR (400 MHz, $C_2D_2Cl_4$, 80 °C): δ 7.63 (s, 4H), 7.56 (dd, 4H, J = 1.8 Hz, J = 6.5 Hz), 7.43 (dd, 4H, J = 1.9 Hz, J = 6.5 Hz), 1.35 (s, 18H) ppm. ^{13}C NMR (100 MHz, $C_2D_2Cl_4$, 80 °C): δ 150.7, 139.7, 137.7, 127.3, 126.8, 126.0, 34.9, 31.6 ppm. FD-MS: 342.9 (100.0). Elemental analysis calculated for $C_{26}H_{30}$: C, 91.17; H, 8.83. Found: C, 91.12; H, 8.99%.

Synthesis of 2,2′-bis(4-*tert*-butylphenyl)-1,1′-biphenyl (4) *via* a non-aqueous microwave procedure

A dried 10 mL microwave tube was charged with 2,2′-dibromo-1,1′-biphenyl (0.04 g, 1,28 mmol), 4-*tert*-butyl-phenylboronic acid (0.091 g, 0.51 mmol), KOH (0.086 g, 1.54 mmol), $Pd(PPh_3)_2Cl_2$ (0.09 g, 0.012 mmol) and sealed under argon with an aluminium cap with a septum. Dry THF (4 mL) was added *via* a syringe and the reaction was irradiated with microwaves (300 W) for 10 min with air-cooling to keep the temperature between 110 and 115 °C. The mixture was poured into water and then extracted with dichloromethane, which was subsequently washed with water and brine, dried over $MgSO_4$ and the solvent was removed by rotary evaporation. The residue was purified by column chromatography on silica gel with hexanes–toluene (95 : 5) as eluent to give **4** in 82% yield. ^{1}H NMR (400 MHz, $C_2D_2Cl_4$, 25 °C): δ 7.42 (dd, 2H, J = 1.6 Hz, J = 7.4 Hz), 7.31 (dtd, 4H, J = 1.5 Hz, J = 7.3 Hz, J = 18.1 Hz), 7.11 (dd, 2H, J = 1.4 Hz, J = 7.5 Hz), 6.87 (d, 4H, J = 8.2 Hz), 6.34 (d, 4H, J = 8.2 Hz), 1.25 (s, 18H) ppm. ^{13}C NMR (100 MHz, $C_2D_2Cl_4$, 32 °C): δ 148.6, 140.9, 140.4, 137.9, 132.1, 129.9, 128.7, 127.8, 127.4, 124.6, 34.5, 31.7 ppm. FD-MS: 418.2 (100.0). Elemental analysis calculated for $C_{32}H_{34}$: C, 91.81; H, 8.19. Found: C, 91.88; H, 8.51%.

Crystal structure determination of compounds 2 and 4

Crystal data for **2**: $C_{52}H_{58}$, Mr = 682.98 g mol^{-1}, colourless, crystal dimensions 0.16 × 0.16 × 0.08 mm, monoclinic *C*2/*c* (no. 15), at 100 K. $a = 26.1849(6)$, $b = 15.8390(4)$, $c = 10.0760(2)$ Å, $\beta = 103.7280(10)°$, $V = 4059.57(16)$ Å^3, $Z = 4$, $D_{calc} = 1.117$ mg m^{-3}, $\mu = 0.062$ mm^{-1}, $\theta_{max} = 31.66°$, 57798 total reflections, 6800 unique, $R_{int} = 0.097$, 241 refined parameter $R = 0.064$, $wR = 0.153$, highest residual electron density peak 0.5 *e* Å^{-3}. Crystal data for **4**: $C_{32}H_{34}$, Mr = 418.59 g mol^{-1}, colourless, crystal dimensions 0.26 × 0.18 × 0.12 mm, monoclinic *P* 21/*c* (no. 14), at 100 K. $a = 7.68070(10)$, $b = 13.23650(10)$, $c = 24.2500(3)$ Å, $\beta = 93.2000(10)°$, $V = 2461.55(5)$ Å^3, $Z = 4$, $D_{calc} = 1.130$ mg m^{-3}, $\mu = 0.471$ mm^{-1}, $\theta_{max} = 69.16°$, 15596 total reflections, 4157 unique, $R_{int} = 0.039$, 296 refined parameters $R = 0.042$, $wR = 0.108$, highest residual electron density peak 0.2 *e* Å^{-3}. CCDC reference numbers: 274217 for **2** and 274216 for **4**.‡

Acknowledgements

B. S. N. thanks the VCI foundation for financial support. The authors thank Ilka Polanz for her assistance with the NMR measurements.

References

1 (*a*) Y. Sun, Y. Liu and D. Zhu, *J. Mater. Chem.*, 2005, **15**, 53; (*b*) G. Horowitz, *J. Mater. Res.*, 2004, **19**, 1946.
2 (*a*) M. T. Berbius, M. Inbasekaran, J. O′Brien and W. S. Wu, *Adv. Mater.*, 2000, **12**, 1737; (*b*) A. Kraft, A. C. Grimsdale and A. B. Holmes, *Angew. Chem., Int. Ed.*, 1998, **37**, 402.
3 M. D. McGehee and A. Heeger, *J. Adv. Mater.*, 2000, **12**, 1655.
4 H. Hoppe and N. S. Sariciftci, *J. Mater. Res.*, 2004, **19**, 1924.
5 A.-D. Schlüter, *Handbook of Conducting Polymers*, Marcel Dekker, New York, 2nd edn., 1998, ch. 8, p. 209.
6 (*a*) U. Scherf and E. List, *Adv. Mater.*, 2002, **14**, 477; (*b*) U. Scherf, *J. Mater. Chem.*, 1999, **9**, 1843.
7 (*a*) K. Müllen, G. Wegner, *Electronic Materials: The Oligomer Approach*, John Wiley & Sons, Weinheim, Germany, 1998; (*b*) R. E. Martin and F. Diederich, *Angew. Chem., Int. Ed.*, 1999, **38**, 1350.
8 Y. Shirota, *J. Mater. Chem.*, 2005, **15**, 75.
9 (*a*) P. Strohriegl and J. V. Grazulevicius, *Adv. Mater.*, 2002, **14**, 1439; (*b*) Y. Shirota, *J. Mater. Chem.*, 2000, **10**, 1.
10 (*a*) J. Li, C. Ma, J. Tang, C.-S. Lee and S. Lee, *Chem. Mater.*, 2005, **17**, 615; (*b*) J. Pei, J.-L. Wang, X.-Y. Cao, X.-H. Zhou and W.-B. Zhang, *J. Am. Chem. Soc.*, 2003, **125**, 9944; (*c*) Y. Geng, A. Fechtenkötter and K. Müllen, *J. Mater. Chem.*, 2001, **11**, 1634.
11 (*a*) H.-J. Su, F.-I. Wu and C.-F. Shu, *Macromolecules*, 2004, **37**, 7197; (*b*) Y. Wu, J. Li, Y. Fu and Z. Bo, *Org. Lett.*, 2004, **6**, 3485; (*c*) W.-J. Shen, R. Dodda, C.-C. Wu, F.-I. Wu, T.-H. Liu, H.-H. Chen, C. H. Chen and C.-F. Shu, *Chem. Mater.*, 2004, **16**, 930; (*d*) T. Spehr, R. Pudzich, T. Fuhrmann and J. Salbeck, *Org. Electron.*, 2003, **4**, 61.
12 (*a*) X.-M. Liu, H. He, J. Huang and J. Xu, *Chem. Mater.*, 2005, **17**, 434; (*b*) X. Deng, A. Mayeux and C. Cai, *J. Org. Chem.*, 2002, **67**, 5279; (*c*) M. R. Robinson, S. Wang, G. C. Bazan and Y. Cao, *Adv. Mater.*, 2000, **12**, 1701.
13 (*a*) A. Almutairi, F. S. Tham and M. J. Marsella, *Tetrahedron*, 2004, **60**, 7187; (*b*) M. J. Marsella, K. Yoon, A. Almutairi, S. K. Butt and F. S. Tham, *J. Am. Chem. Soc.*, 2003, **125**, 13928; (*c*) A. J. Blake, P. A. Cooke, K. J. Doyle, S. Gair and N. S. Simpkins, *Tetrahedron Lett.*, 1998, **39**, 9093; (*d*) L. Tong, H. Lau, D. M. Ho and R. A. Pascal, Jr., *J. Am. Chem. Soc.*, 1998, **120**, 6000.
14 B. S. Nehls, S. Füldner, E. Preis, T. Farrell and U. Scherf, *Macromolecules*, 2005, **38**, 687.
15 CEM Discovery single mode focused microwave.
16 The related unsubstituted 2,5,2′,5′-terphenyl-1,1′-biphenyl has been prepared by an alternative method. E. Ibuki, S. Ozasa, Y. Fugioka and H. Kitamura, *Chem. Pharm. Bull.*, 1980, **28**, 1468.
17 E. E. Hagberg, D. E. Olson and V. V. Sheares, *Macromolecules*, 2004, **37**, 4748.
18 (*a*) K. R. Carter, *Macromolecules*, 2002, **35**, 6757; (*b*) T. Yamamoto, Y. Fugiwara, H. Fukumoto, Y. Nakamura, S. Koshihara and T. Ishikawa, *Polymer*, 2003, **44**, 4487.
19 C. A. Hunter and J. K. M. Sanders, *J. Am. Chem. Soc.*, 1990, **112**, 5525.
20 C. Janiak, *J. Chem. Soc., Dalton Trans.*, 2000, **112**, 3885.
21 K. M. Guckian, B. A. Schweitzer, R. X.-F. Ren, C. J. Sheils, D. C. Tohmassebi and E. T. Kool, *J. Am. Chem. Soc.*, 2000, **122**, 2213.
22 (*a*) R. El Abed, B. Ben Hassine, J.-P. Genêt, M. Gorsane and A. Marinetti, *Eur. J. Org. Chem.*, 2004, **122**, 1517; (*b*) J. E. Field, T. J. Hill and D. Venkataraman, *J. Org. Chem.*, 2003, **68**, 6071; (*c*) K. Paruch, L. Vyklický, T. J. Katz, C. D. Incarvito and A. L. Rheingold, *J. Org. Chem.*, 2000, **65**, 8774.
23 (*a*) T. Nakano and T. Yade, *J. Am. Chem. Soc.*, 2003, **125**, 15474; (*b*) R. Rathore, S. H. Abelwahed and I. A. Guzei, *J. Am. Chem. Soc.*, 2003, **125**, 8712.
24 Recent examples include: (*a*) A. Orita, T. Nakano, D. Lie An, K. Tanikawa, K. Wakamatsu and J. Otera, *J. Am. Chem. Soc.*, 2004, **126**, 10389; (*b*) D. J. Hill, M. J. Mio, R. B. Prince, T. S. Hughes and J. S. Moore, *Chem. Rev.*, 2001, **101**, 3893; (*c*) H. Masu, M. Sakai, K. Kishikawa, M. Yamamoto, K. Yamaguchi and S. Kohmoto, *J. Org. Chem.*, 2005, **70**, 1423; (*d*) D. Zhao and J. S. Moore, *J. Org. Chem.*, 2002, **67**, 3548; (*e*) M. S. Cubberly and B. L. Iverson, *J. Am. Chem. Soc.*, 2001, **123**, 7560; (*f*) T. J. Katz, *Angew. Chem., Int. Ed.*, 2000, **39**, 1921; (*g*) L. A. Cuccia, J.-M. Lehn, J.-C. Homo and M. Schmutz, *Angew. Chem., Int. Ed.*, 2000, **39**, 233; (*h*) R. B. Prince, T. Okada and J. S. Moore, *Angew. Chem., Int. Ed.*, 1999, **38**, 233; (*i*) A. E. Rowan and R. J. M. Nolte, *Angew. Chem., Int. Ed.*, 1998, **37**, 63.
25 (*a*) I. B. Berlman, H. O. Wirth and O. Steingraber, *J. Phys. Chem.*, 1971, **75**, 318; (*b*) I. B. Berlman, *J. Chem. Phys.*, 1970, **52**, 5616.
26 G. B. Schuster, *Acc. Chem. Res.*, 2000, **33**, 253.

‡ CCDC reference numbers 274216 and 274217. See http://dx.doi.org/10.1039/b508125d for crystallographic data in CIF or other electronic format.